ASPECTS OF ELECTRONIC STRUCTURE INSTABILITY IN SEARCH FOR NEW SUPERCONDUCTORS: SUPERCONDUCTING BORIDE AT LIQUID NITROGEN TEMPERATURE?

Pavol BAŇACKÝ[a,b]

[a] *Institute of Chemistry, Chemical Physics Division, Faculty of Natural Science, Comenius University, Mlynská dolina CH2, 842 15 Bratislava, Slovakia; e-mail: banacky@fns.uniba.sk*

[b] *S-Tech a.s., Dúbravská cesta 9, 841 05 Bratislava, Slovakia*

Received April 7, 2008
Accepted June 24, 2008
Published online September 17, 2008

Dedicated to Professor Rudolf Zahradník on the occasion of his 80th birthday.

It has been shown that electron-phonon coupling in superconductors induces temperature-dependent electronic structure instability which is related to fluctuation of analytic critical point of some bands across the Fermi level. The band fluctuation results in a considerable reduction of chemical potential and to breakdown of the adiabatic Born–Oppenheimer approximation. At critical temperature T_c, superconducting system undergoes transition from the adiabatic electronic ground state into the antiadiabatic state at broken symmetry, which is stabilized due to the effect of nuclear dynamics. This effect is absent in non-superconducting compounds. In a good agreement with the experimental T_c of superconducting state transition, the critical temperature of the adiabatic ↔ antiadiabatic state transition has been calculated for three different superconductors. Two hypothetical compounds, LiB and ZnB_2, are predicted to be potential superconductors with T_c about 17 and 77.5 K, respectively.

Keywords: Antiadiabatic state; Nonadiabatic electron-phonon interactions; Superconductors.

Progress in synthesis of new superconductors based on empirical approaches is rather slow. Identification of some aspect of the electronic band structure that is common to superconductors and that is absent in respective non-superconducting analogues should be of crucial importance in quest for new superconductors. In the present work such aspect is specified and theoretical treatment of the adiabatic ↔ antiadiabatic state transition which could be a predictive tool for design of new superconductors is presented.

Collect. Czech. Chem. Commun. 2008, Vol. 73, Nos. 6–7, pp. 795–810

doi:10.1135/cccc20080795

Results of angle-resolved photoemission spectroscopy (ARPES) for a wide group of cuprate superconductors[1] have disclosed the formation of a kink on the momentum distribution curve close to the Fermi level (FL) and it has been found[2,3] that formation of the giant kink at FL is temperature-dependent. It is present at temperatures below T_c and disappears above it. These results indicate the importance of electron–phonon (EP) interactions also for superconductivity in cuprates, and moreover this kind of temperature dependence is strong indication of possible electronic structure instability in the transition to superconducting state in general.

In the present work it is shown that the indicated instability can be identified in electronic structure of different superconductors in coupling to respective phonon mode(s) pertaining to a particular superconducting material. The electronic structure instability is associated with a sudden, temperature-related, transition from the adiabatic electronic ground state into the antiadiabatic electronic ground state, which is stabilized below T_c at broken symmetry with respect to the adiabatic high-symmetry structure. The antiadiabatic state is geometrically degenerate, with fluxional nuclear configuration in the phonon mode(s) that drive this transition. Electronic structure calculation and band structure (BS) topology provide under these circumstances physical parameters for identification and characterization of superconducting state.

ELECTRONIC STRUCTURE INSTABILITY – FORMATION OF ANTIADIABATIC STATE

Preliminaries

Crystal structures of the studied compounds are different, with the exception of ZnB_2 which is assumed to be of the same hexagonal type as MgB_2 (hP3, *P6mmm*, No. 191; AlB_2 ω-type) (Fig. 1a). Cubic structure (cP7, *Pm3m*, No. 221; CaB_6 type) is characteristic of YB_6 (Fig. 1b). Monoboride LiB is assumed in a graphite-like structure (hP4, $P6_3mmc$, No. 194) with alternating B and Li honeycomb layers (Fig. 1c). The $YBa_2Cu_3O_7$ is orthorhombic (oP14, *Pmmm*, No. 47, with chain oxygen in *b*-direction and vacancy in *a*-direction) (Fig. 1d).

The band structures have been calculated by computer code Solid2000. The code is based on the Hartree–Fock SCF method for infinite periodic cyclic 3D cluster[4] with the quasi-relativistic INDO Hamiltonian[5]. Based on the results of atomic Dirac–Fock calculations[6], the INDO version used in the SOLID package is parametrized for nearly all elements of the Periodic chart. Incorporating the INDO Hamiltonian into the cyclic cluster method

(with Born–Karman boundary conditions) for electronic band structure calculations has many advantages and some drawbacks as well. The method is not very convenient for strong ionic crystals but it yields good results for intermediate ionic and covalent systems. The main disadvantage is an overestimation of the total width of bands. On the other hand, it yields satisfactory results for properties related to electrons at the Fermi level (frontier-orbital properties) and for calculation of equilibrium geometries[7–9].

In practical calculations, the basic cluster of the dimension $N_a \times N_b \times N_c$, is generated by corresponding translations of the unit cell in the directions of crystallographic axes, a (N_a), b (N_b), c (N_c). In particular, the band structure calculations have been performed for the basic clusters 11 × 11 × 7 for MgB_2 (ZnB_2), 15 × 15 × 15 for LiB, 9 × 9 × 9 for YB_6 and 5 × 5 × 5 for $YBa_2Cu_3O_7$. The scaling parameter 1.2 has been used in calculations of the one-electron off-diagonal two-center matrix elements of the Hamiltonian (β-"hopping" integrals). The basic cluster of the particular size generates a

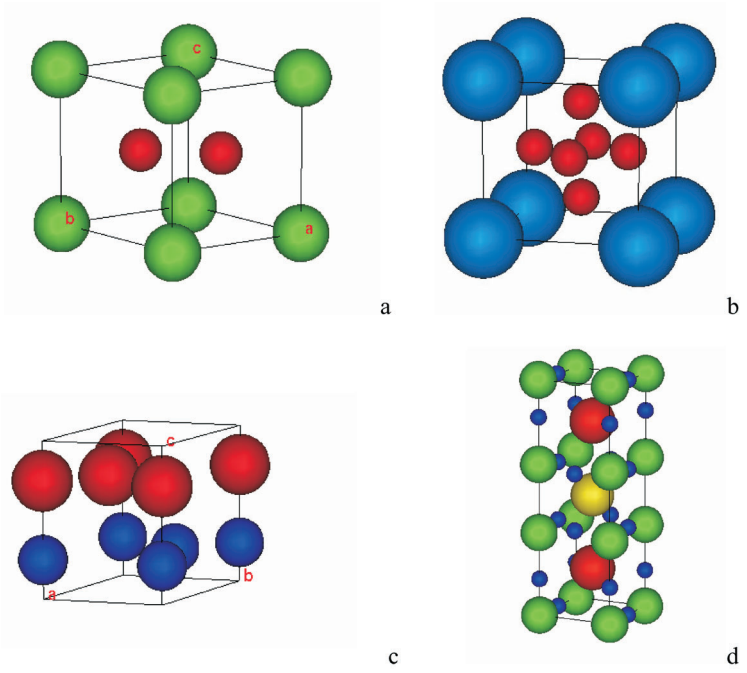

FIG. 1
Crystallographic cells of MgB_2 and ZnB_2 (a), YB_6 (b), LiB (c) and $YBa_2Cu_3O_7$ (d)

grid of ($N_a \times N_b \times N_c$) points in *k*-space. The HF-SCF procedure is performed for each *k*-point of the grid with the INDO Hamiltonian matrix elements that obey the boundary conditions of the cyclic cluster[4]. The Pyykko–Lohr quasi-relativistic basis set of the valence electron atomic orbitals (s,p-AO for Li, B, Ba, O, Zn and s,p,d-AO for Cu and Y) has been used. In the case of $YBa_2Cu_3O_7$, for instance, there is 13 atoms and 72 AO/unit cell. The basic cluster 5 × 5 × 5 with 1625 atoms generates a grid of 125 points in *k*-space; the total number of STO-type functions in the cluster is 9000. In the case of MgB_2 (ZnB_2), the unit cell has 3 atoms and 12 AO. In the basic cluster 11 × 11 × 7, there are 2541 atoms with the total number 10164 STO-type functions and the generated grid has 847 points in *k*-space. The number of STO-type functions is unambiguously determined by the number of AO of the valence electrons pertaining to atoms which constitute the basic cluster. Dimension of the basic cluster directly determines the number of generated *k*-points in the grid, $N_a \times N_b \times N_c$. In general, the precision of the results of band structure calculation increases with increasing dimension of the basic cluster. It has been shown[4,7–9], however, that there is an effect of saturation, a bulk limit beyond which the effect of increasing dimension on, e.g., total electronic energy, orbital energies, HOMO-LUMO difference, is negligibly small. In practice, dimension of the basic cluster and parameters selection (e.g., for calculation of β integrals) is a matter of reasonable compromise between computational efficiency and compatibility of calculated electronic properties and equilibrium geometry with respect to some reference or experimental data. It should be kept in mind, however, that the basic efficiency and accuracy are restricted by the INDO method parametrization.

Band Structures

In Fig. 2 (a, c, e, g, i – the pictures on the left), there are BS of the studied compounds with optimized equilibrium geometries. Three of them are well-known superconductors with BS presented in Fig. 2 (a, b), (c, d), (e, f). The BS of hypothetical structures (LiB, ZnB_2), which are predicted in this work to be superconducting, are presented in Fig. 2 (g, h) and (i, j).

All the band structures are of adiabatic metal-like character with a relatively low density of states at the FL (indicated by a dashed line). Coupling to the respective phonon mode(s) in particular compounds seemingly does not change the metal-like character of BS. In all cases, however, EP coupling induces BS fluctuation (see the pictures on the right), which is charac-

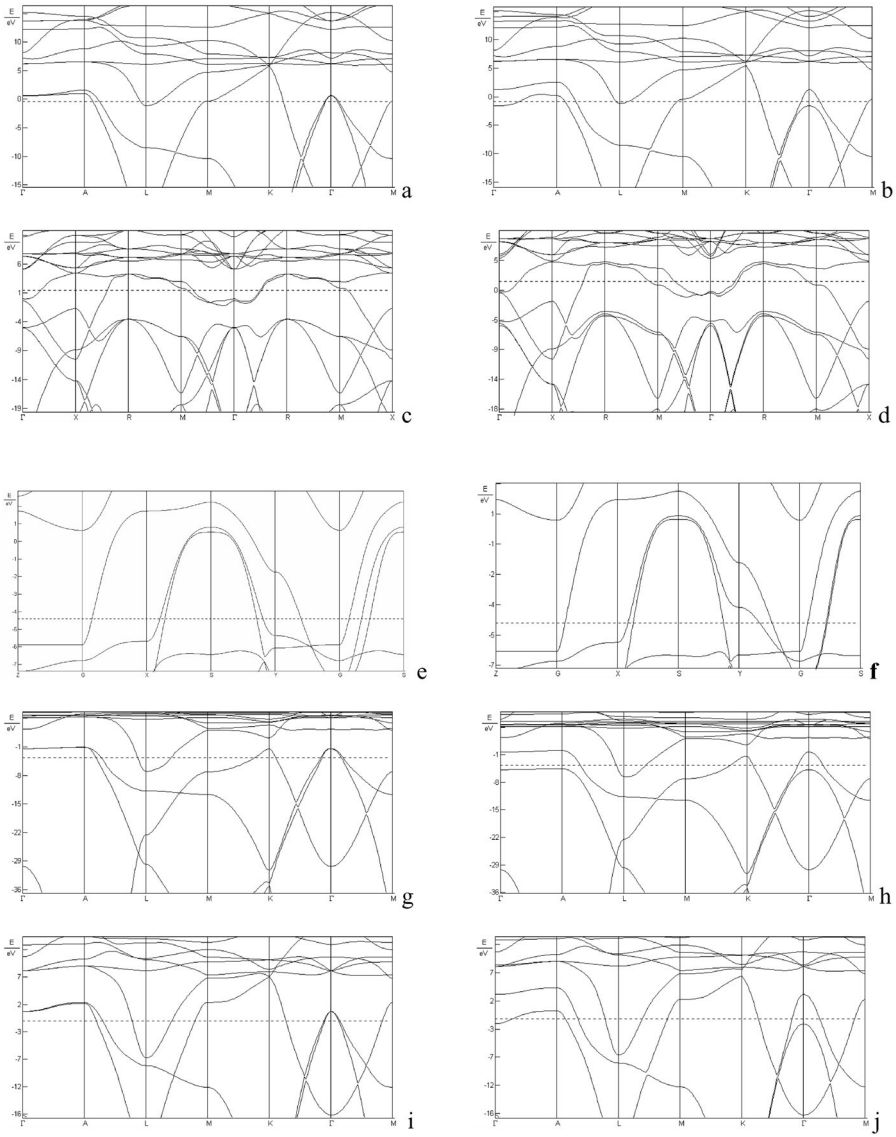

FIG. 2

Band structures of MgB_2 (a, b), YB_6 (c, d), $YBa_2Cu_3O_7$ (e, f), LiB (g, h) and ZnB_2 (i, j). Pictures on the left (a, c, e, g, i) correspond to equilibrium high-symmetry structures; on the right (b, d, f, h, j) are the band structures of distorted geometry with atom displacements in the respective phonon modes

teristic by fluctuation of the analytical critical point (ACP) of some band across FL (cf. a–b, c–d, e–f, g–h, i–j).

In particular, for MgB_2 coupling to the E_{2g} phonon mode (in-plane stretching vibration of B–B) results in splitting of σ bands (p_x, p_y electrons of B atoms in *a–b* plane) in Γ point of the first Brillouin zone (BZ) (Fig. 2b). Related to band topology, the analytic critical point (ACP, maximum) of σ bands is located at Γ point and, for the displacement ≈0.016 Å/B-atom out of equilibrium position, the ACP crosses FL. This means periodic fluctuation of the BS between topologies 2a ↔ 2b in coupling to vibration in the E_{2g} mode.

The situation is similar for YB_6. In this case, BS fluctuation is related to the T_{2g} mode (valence vibration of B atoms in basal *a–b* plane of B-octahedron). At the displacement ≈0.017 Å/B-atom out of equilibrium position, the ACP (saddle point) of the band with dominance of B-p and Y-d electrons crosses FL in the M point and the BS fluctuates between topologies 2c ↔ 2d.

In the case of $YBa_2Cu_3O_7$, the BS fluctuation is associated with coupling to three modes, A_g, B_{2g}, B_{3g}, with the apical O(4) and CuO-plane O(2), O(3) atom displacements. At displacements ≈0.031 Å of apical O(4) in the A_g mode and ≈0.022 Å of O(2) and O(3) in the B_{2g}, B_{3g} modes, the ACP (saddle point) of one of the Cu–O plane (d-pσ) band in Y point crosses FL and undergoes periodic fluctuation between topologies 2e ↔ 2f.

Coupling to B-stretching in LiB induces FL crossing of ACP (maximum) of the σ band in Γ point at displacement ≈0.026 Å/B-atom and undergoes periodic fluctuation of BS between topologies 2g ↔ 2h in vibration motion.

The situation for ZnB_2 is nearly the same as for MgB_2. The difference is only in the value of displacement, which is now ≈0.03 Å/B-atom, at which ACP (maximum) of σ band crosses FL in Γ point. The BS fluctuates between topologies 2i ↔ 2j.

Nonadiabatic Effects

Formation of Antiadiabatic Ground State and Gap Opening

Splitting of the σ bands in coupling to the E_{2g} mode in MgB_2 has been reported[10] in 2001 but no special attention has been paid to this effect. Shortly after, superconductivity of MgB_2 has been straightforwardly interpreted[11] as a standard strong coupling BCS-like character. As it has been mentioned, for its clumped nuclear equilibrium structure, the BS is of the

adiabatic metal-like character; the Fermi energy E_F^σ of σ band electrons (i.e., chemical potential μ) is ca. 0.5 eV, which is great enough compared with the vibration energy of the E_{2g} phonon mode – $\omega_{2g} \approx 0.07$ eV.

Nevertheless, the matter is more complicated. It has been shown[12,13] that ACP crosses FL at displacement ≈0.016 Å, which is smaller than root-mean square (rms) displacement (≈0.036 Å) for zero-point vibration energy in the E_{2g} mode. This means, however, that in vibration where ACP approaches FL at the distance less than ±ω, the adiabatic Born–Oppenheimer approximation (BOA) is not valid and standard adiabatic theories (including calculation of vertex corrections, e.g., ref.[14]) cannot be applied. In this case, Fermi energy E_F^σ of σ band electrons (chemical potential μ) close to Γ point is smaller than the E_{2g} mode vibration energy $E_F^\sigma < \omega_{2g}$. Moreover, the ACP shift substantially increases the density of states (DOS) at FL, $n_\sigma(E_F) = (\partial\varepsilon_\sigma^0 / \partial k)_{E_F}^{-1}$, and induces the corresponding decrease in the effective electron velocity $(\partial\varepsilon_\sigma^0 / \partial k)_{E_F}$ of fluctuating band in this region of *k*-space. Under these circumstances, the system is in the intrinsic nonadiabatic state, or even in the antiadiabatic state, $E_F^\sigma << \omega_{2g}$, and electronic motion depends not only on nuclear coordinates *Q* but is strongly influenced by nuclear dynamics – momenta *P*. The main part of the effect of nuclear kinetic energy on electronic motion can be derived as diagonal correction by sequential *Q*,*P*-dependent base transformations (or quasi-particle transformation[15]). This is a generalization of adiabatic *Q*-dependent transformation which yields the well-known adiabatic diagonal BO correction[16,17] (DBOC). Due to diagonal approximation with the factorized form of total wave function, $\Psi_0(r,Q,P) = \Phi_0(r,Q,P)\ X_0(Q,P)$, the standard clumped nuclear Hamiltonian treatment can be used and the *Q*,*P*-effect is calculated in the form of corrections to the electronic ground-state energy (zero-particle term correction), corrections to orbital energies (one-particle term corrections) and two-particle term corrections (correction to the electron correlation energy).

Correction to the electronic ground-state energy in the *k*-space representation due to interaction of pair of states mediated by the phonon mode *r* can be written as

$$\Delta E^0_{(\mathrm{na})} = 2\sum_{\varphi_{Rk}}\sum_{\varphi_{Sk'}}\int_0^{\varepsilon_{k',\max}} n_{\varepsilon_{k'}}(1-f_{\varepsilon^0 k'})\,\mathrm{d}\varepsilon^0_{k'}\int_{\varepsilon_{k,\min}}^{\varepsilon_{k,\max}} f_{\varepsilon^0 k}|u^r_{k-k'}|^2\, n_{\varepsilon_k}\frac{\hbar\omega_r}{(\varepsilon^0_k-\varepsilon^0_{k'})^2-(\hbar\omega_r)^2}\,\mathrm{d}\varepsilon^0_k, \qquad (1)$$

$$\varphi_{Rk} \neq \varphi_{Sk'}\ .$$

In general, all bands of 1st BZ of a multiband system are covered, including intraband terms, i.e., φ_{Rk}, $\varphi_{Rk'}$, $k \neq k'$, while $\varepsilon_k^0 < \varepsilon_F$, $\varepsilon_{k'}^0 > \varepsilon_F$. Fermi–Dirac populations $f_{\varepsilon^0 k}$, $f_{\varepsilon^0 k'}$ make correction (*1*) temperature-dependent. Term $u_{k-k'}^r$ stands for matrix element of EP coupling and $n_{\varepsilon k}$, $n_{\varepsilon k'}$ are DOS of interacting bands at $\varepsilon_{k'}^0$ and ε_k^0. For adiabatic systems, such as metals, this correction is positive and negligibly small (DBOC). Only for systems in the antiadiabatic state the correction is negative and its absolute value depends on the magnitudes of $u_{k-k'}^r$ and $n_{\varepsilon k}$, $n_{\varepsilon k'}$ at displacement for FL crossing. At the moment when ACP approach FL, the system not only undergoes transition to the antiadiabatic state but DOS of the fluctuating band is considerably increased at FL.

For all the presented systems at 0 K, $\Delta E_{(na)}^0$, which covers the effect of nuclear momenta, prevails in absolute value the electronic energy increase $\Delta E_{cr} = E_{d,cr} - E_{eq}$ at nuclear displacements d_{cr} when ACP crosses FL as calculated for clumped nuclear adiabatic structures. Under these circumstances, the system is stabilized in the antiadiabatic electronic ground state at broken symmetry with respect to the adiabatic equilibrium high-symmetry structure. It can be identified by ARPES as a kink on momentum distribution curve at FL, i.e., as band curvature at ACP when approaching FL – see the calculated results for $YBa_2Cu_3O_7$ (Fig. 3).

Due to translation symmetry of the lattice, the created antiadiabatic electronic ground state is geometrically degenerate in distorted geometry with fluxional nuclear configuration in particular phonon mode(s) – see, e.g., Fig. 2 in ref.[12]. The ground state energy is the same for different positions of the involved atoms (in phonon modes which drive the system into this

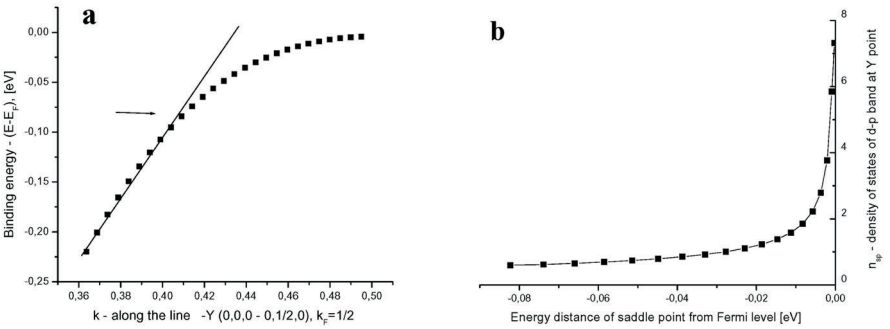

FIG. 3
Calculated dispersion of d-pσ band in Γ–Y direction with the kink formation indicated by the arrow (a) and increase in the d-pσ band DOS when ACP approaches FL (b) for $YBa_2Cu_3O_7$

state) at circulation over perimeters of circles with radii equal to displacements d_{cr} at FL crossing.

In transition to the antiadiabatic state, k-dependent gap $\Delta_k(T)$ in quasicontinuum of adiabatic one-electron spectrum is opened. The gap opening is related to shift $\Delta\varepsilon_{Pk}$ of the original adiabatic orbital energies ε^0_{Pk}, $\varepsilon_{Pk} = \varepsilon^0_{Pk} + \Delta\varepsilon_{Pk}$, and to the k-dependent change of DOS of particular band(s) at Fermi level. Shift of orbital energies in band $\varphi_P(k)$ has the form

$$\Delta\varepsilon(Pk') = \sum_{Rk'_1 > k_F} |u^{k'-k'_1}|^2 \, (1 - f_{\varepsilon^0 k'_1}) \frac{\hbar\omega_{k'-k'_1}}{(\varepsilon^0_{k'} - \varepsilon^0_{k'_1})^2 - (\hbar\omega_{k'-k'_1})^2} -$$

$$- \sum_{Sk < k_F} |u^{k'-k'_1}|^2 \, f_{\varepsilon^0 k} \frac{\hbar\omega_{k-k'}}{(\varepsilon^0_{k'} - \varepsilon^0_{k})^2 - (\hbar\omega_{k-k'})^2} \qquad (2)$$

for $k' > k_F$, and

$$\Delta\varepsilon(Pk) = \sum_{Rk'_1 > k_F} |u^{k-k'_1}|^2 \, (1 - f_{\varepsilon^0 k'_1}) \frac{\hbar\omega_{k-k'_1}}{(\varepsilon^0_{k} - \varepsilon^0_{k'_1})^2 - (\hbar\omega_{k-k'_1})^2} -$$

$$- \sum_{Sk_1 < k_F} |u^{k-k_1}|^2 \, f_{\varepsilon^0 k} \frac{\hbar\omega_{k-k_1}}{(\varepsilon^0_{k} - \varepsilon^0_{k_1})^2 - (\hbar\omega_{k-k_1})^2} \qquad (3)$$

for $k \le k_F$.

Replacement of discrete summation by integration, $\Sigma_k \ldots \rightarrow \int n(\varepsilon_k)$, introduces DOS $n(\varepsilon_k)$ into Eqs (*2*) and (*3*), which is of crucial importance in relation to fluctuating band (Fig. 3b). For corrected DOS $n(\varepsilon_k)$, which is the consequence of shift $\Delta\varepsilon_k$ of orbital energies, the following relation can be derived:

$$n(\varepsilon_k) = |1 + (\partial(\Delta\varepsilon_k) / \partial\varepsilon^0_k)|^{-1} \, n^0(\varepsilon^0_k) \, . \qquad (4)$$

Term $n^0(\varepsilon^0_k)$ stands for uncorrected DOS of the original adiabatic states of particular band,

$$n^0(\varepsilon^0_k) = |(\partial\varepsilon^0_k / \partial k)|^{-1} . \qquad (5)$$

Close to the *k*-point where the original band that interacts with fluctuating band intersects FL, the occupied states near FL are shifted downward below FL and unoccupied states are shifted upward above FL. The gap is identified as the energy distance between created peaks in corrected DOS above FL (half-gap) and below FL. The formation of peaks is related to the spectral weight transfer that is observed by ARPES or tunneling spectroscopy in cooling below T_c.

For the studied compounds, the calculated corrected DOS of particular band(s) with gap opening are given in Fig. 4. In particular, $YBa_2Cu_3O_7$ exhibits an asymmetric gap in two directions: O1-pσ band gap is $\Delta_b(0) \approx$ 35.7 meV in the Γ–Y direction (Fig. 4a) and $\Delta_a(0) \approx 24.2$ meV in the Γ–X direction (Fig. 4b). The calculated asymmetry, i.e., the ratio $(\Delta_a(0)/\Delta_b(0))_{theor} \approx$ 0.68 is very close to the experimental value (≈0.66) that has been recorded[18] for untwined $YBa_2Cu_3O_7$.

Two gaps, on σ and π bands, are formed in Γ–K(M) directions of MgB_2 (Fig. 4c): $\Delta_\sigma(0)/2 \approx 7.6$ meV and $\Delta_\pi(0)/2 \approx 2.2$ meV. The result simulates tunneling spectra at positive bias voltage and calculated half-gaps are in a very good agreement with experimental high-precision measurements[19,20].

A small gap opens on pd-band in the Γ–X direction of YB_6 (Fig. 4d): $\Delta_{pd}(0)/2 \approx 2.2$ meV.

Two gaps, related to σ and π bands in Γ–K(M) directions, are expected for LiB (Fig. 4e): $\Delta_\sigma(0)/2 \approx 3.3$ meV and $\Delta_\pi(0)/2 \approx 2.0$ meV. Considerably larger gaps are opened for ZnB_2 on σ and π bands in Γ–K(M) directions (Fig. 4f): $\Delta_\sigma(0)/2 \approx 14.9$ meV and $\Delta_\pi(0)/2 \approx 8.7$ meV.

The corrections to orbital energies (*2*), (*3*) and to the ground state energy (*1*) are temperature dependent and decrease with increasing *T*. At a critical value T_c, the gap in one-particle spectrum[21],

$$\Delta(T) = \Delta(0)\ \mathrm{tgh}\,(\Delta(T)/4k_BT), \qquad (6)$$

that is formed at 0 K, disappears, $\Delta(T_c) = 0$ (continuum of states is established at FL), while $|\Delta E^0_{(na)}(T_c)| \le \Delta E_{d,cr}$ and the system undergoes transition from the antiadiabatic into adiabatic state, which is stable for equilibrium high-symmetry structure above T_c. With respect to Δ(0), a simple approximate relation follows from Eq. (*6*)

$$T_c = \Delta(0)/4k_B\,. \qquad (7)$$

The calculated values of T_c for presented compounds are: $YBa_2Cu_3O_7$, $T_c \approx 92.8$ K; MgB_2, $T_c \approx 39.5$ K; YB_6, $T_c \approx 11$ K. It is in a good agreement with experimental values of T_c for superconducting state transition of particular compounds[22–24].

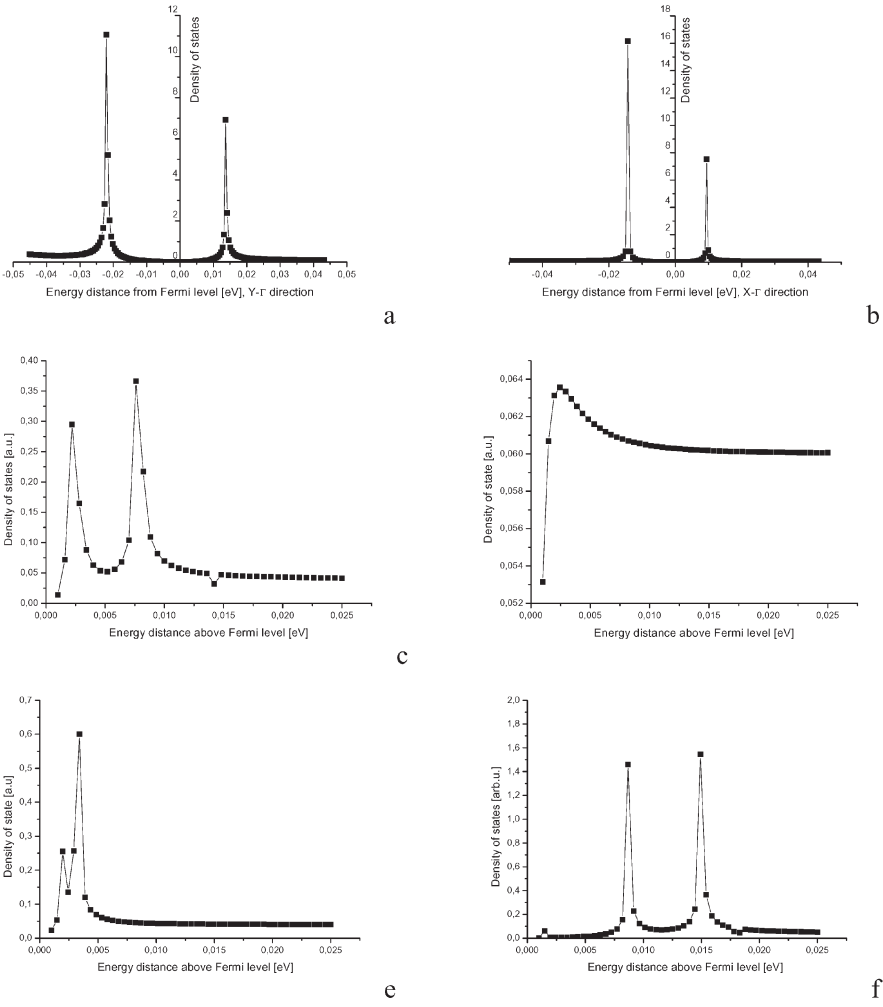

FIG. 4
Corrected DOS and gap formation near *k*-point where particular bands intersect FL, 0 K

However, it should be noticed that while there is a general consensus about importance of the EP coupling to the A_g, B_{2g}, B_{3g} and E_{2g} phonon modes in case of $YBa_2Cu_3O_7$ and MgB_2 in transition to superconducting state, the situation with YB_6 is rather controversial. Recent studies[25,26] advocate importance of EP coupling to low-frequency (8–10 meV) phonon modes of Y-vibration for superconducting coupling. It is associated with overall value of dimensionless EP coupling constant λ for calculation of T_c according to McMillan formula. For medium-strong coupling $\lambda \approx 1$–1.4 and Coulomb pseudopotential $\mu^* \approx 0.1$–0.2, the experimental $T_c \approx 6.2$–9 K is reproduced. At these circumstances, low-frequency Y-vibrations contribute by 84% to the overall value of λ. Our results show, however, that coupling to Y-vibration does not induce the adiabatic-antiadiabatic state transition. This transition is connected to B-vibrations, in particular to T_{2g} mode. The value of dimensionless constant λ related to T_{2g} mode coupling, calculated in our study is, $\lambda_{T2g} \approx 0.1$. This value is in full agreement with decomposition of Eliashberg spectral function on contributions from the particular phonon modes in YB_6 calculated by Schell et al.[27]. The overall value of $\lambda \approx 0.48$ that accounts for nonlocal corrections on EP coupling in the modes where B-octahedras move as a whole is dominated by high-frequency (30–90 meV) B-vibrations. The authors[27] made conclusion that in transition to superconducting state in YB_6, the B-vibration phonon modes are essential. The conclusion is based on the fact that within McMillan formula, a small increase in overall $\lambda \approx 0.48$ can reproduce experimental T_c. In the present work, it is shown that in spite of the fact that coupling to T_{2g} mode is weak ($u^{k-k'} \approx 0.1$ eV), transition in superconducting state and relatively high value of T_c can be reached due to enormous increase of DOS of the fluctuating band in M point at EF, from the adiabatic value 0.06 states/eV to the value 1.09 states/eV at transition into antiadiabatic state.

With respect to present results, it can be expected that LiB and ZnB_2, when synthesized, will also be superconductors. The calculated T_c for LiB is 17 K. Comparable value of T_c (7–15 K), based on similarity of equilibrium (adiabatic) band structures of LiB and MgB_2, has been predicted within the BCS frame for this compound recently[28,29], even for crystal structure different from that presented here.

So far there has been no prediction for ZnB_2. This compound should be superconductor with $T_c \approx 77.5$ K as it follows from present results. Even the theoretical value of the formation energy of ZnB_2 is slightly positive, under proper synthetic conditions and high pressures it is quite realistic to expect that this compound could be prepared.

Instability of the electronic structure is absent in respective non-superconducting analogues, such as $YBa_2Cu_3O_6$, CaB_6 (insulator), XB_2 (X = Al, Sc, Y, Ti, Zr, Hf, V, Nb, Ta, Cr, Mo, W, Mn, ...). Even in the case of the XB_2, coupling to the E_{2g} mode induces splitting of σ bands in the Γ point, the systems remain stable in the adiabatic state. For these systems, the ACP of σ band does not fluctuate across FL. As an illustration, in Fig. 5 are given band structures of AlB_2 at equilibrium high-symmetry structure (Fig. 5a) and at distorted geometry (Fig. 5b) with the same B-atom displacements in the E_{2g} phonon mode as in the case of MgB_2 in the transition to the superconducting state. In spite of σ bands splitting and nearly the same value of the EP interaction strength (the calculated mean value is $\bar{u} \approx$ 1.01 eV/u cell) as that of MgB_2 ($\bar{u} \approx 0.98$ eV/u cell), AlB_2 remains in EP coupling in the adiabatic state as a non-superconducting compound. In this case, BS fluctuation (bands splitting in EP coupling) does not decrease chemical potential, it remains in EP coupling still larger than the vibration energy ($\mu_{ad} > \hbar\omega$) and, consequently, there is no driving force for transition to the antiadiabatic state.

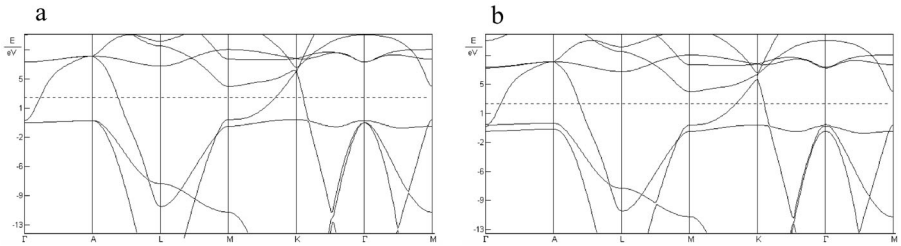

FIG. 5
Band structure of AlB_2 at equilibrium geometry (a) and at distorted geometry (b)

In the case of deoxygenated[30] YBCO – $YBa_2Cu_3O_6$, in contrast to the superconducting $YBa_2Cu_3O_7$, a combination of electron coupling to the A_g, B_{2g} and B_{3g} phonon modes leaves band structure without substantial change (Fig. 6). In the case of $YBa_2Cu_3O_7$, the SP at Y point fluctuates across FL (see Fig. 2e and 2f), which yields substantial reduction of chemical potential $\rightarrow \mu_{antiad} < \hbar\omega$. For $YBa_2Cu_3O_6$ the SP does not fluctuate across FL and chemical potential remains larger than the phonon energy spectrum, $\mu_{ad} > \hbar\omega$, and the system remains in the adiabatic state.

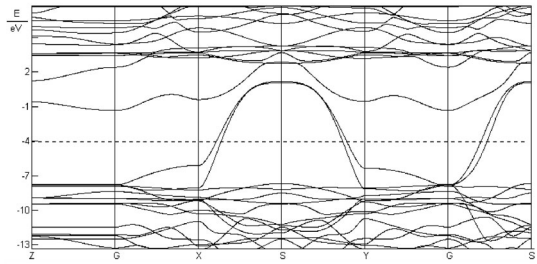

FIG. 6
Band structure of $YBa_2Cu_3O_6$ with equilibrium high-symmetry structure remains without substantial change also at distorted geometry with O(4), O(2) and O(3) atom displacements in the A_g, B_{2g} and B_{3g} phonon modes

CONCLUSIONS

Based on the obtained results, it can be concluded that EP coupling in superconductors induces the temperature-dependent electronic structure instability related to fluctuation of ACP of some band across FL, which results in breakdown of the adiabatic BOA. When ACP approaches FL, chemical potential μ_{ad} is substantially reduced to μ_{antiad} ($\mu_{ad} >> \mu_{antiad} < \hbar\omega$). Under these circumstances the system is stabilized due to the effect of nuclear dynamics, in the antiadiabatic state at broken symmetry with a gap in one-particle spectrum. With increasing T, the stabilization effect of nuclear kinetic energy decreases and at critical temperature T_c the gap(s) extinct and system is stabilized in the adiabatic metal-like state with a continuum of states at FL, which is characteristic by high-symmetry structure. For the studied superconductors, $YBa_2Cu_3O_7$, MgB_2 and YB_6, the calculated T_c of electronic state transition is in a good agreement with experimental values of T_c for the superconducting state transition. Instability of the electronic structure is absent in respective non-superconducting analogues, e.g., $YBa_2Cu_3O_6$, CaB_6 (insulator), XB_2 (X = Al, Sc, Y, Ti, Zr, Hf, V, Nb, Ta, Cr, Mo, W, Mn, ...). Even in the case of XB_2, coupling to the E_{2g} mode induces σ bands splitting in the Γ point, the systems remain stable in the adiabatic state – the ACP of σ band does not fluctuate across FL. The situation is different for hypothetical LiB and ZnB_2 which are predicted to be superconductors and ZnB_2 should be superconducting at temperature of liquid nitrogen.

The author acknowledges financial support of S-Tech Co, as well as support by the grant VEGA1/0013/08.

REFERENCES

1. Lanzara A., Bogdanov P. V., Zhou X. J., Kellar S. A., Feng D. L., Lu E. D., Yoshida T., Eisaki H., Fujimori A., Kishio K., Shimoyama J. I., Noda T., Uchida S., Hussain Z., Shen Z. X.: *Nature* **2001**, *412*, 510.
2. Lanzara A., Bogdanov P. V., Kellar S. A., Zhou X. J., Lu E. D., Gu G., Shimoyama I., Kishio I., Hussain Z., Shen Z. X.: *J. Phys. Chem. Solids* **2001**, *62*, 21.
3. Takahashi T., Sato T., Matsui H., Terashima K.: *New J. Phys.* **2005**, *7*, 105.
4. Noga J., Baňacký P., Biskupič S., Boča R., Pelikán P., Zajac A.: *J. Comput. Chem.* **1999**, *20*, 253.
5. Pople J. A., Beveridge D. L.: *Approximate Molecular Orbital Theory*. McGraw–Hill Inc, New York 1970.
6. a) Boča R.: *Int. J. Quantum Chem.* **1987**, *31*, 941; b) Boča R.: *Int. J. Quantum Chem.* **1988**, *34*, 385.
7. Zajac A., Pelikán P., Noga J., Baňacký P., Biskupič S., Svrček M.: *J. Phys. Chem. B* **2000**, *104*, 1708.
8. Zajac A., Pelikán P., Minár J., Noga J., Straka M., Baňacký P., Biskupič S.: *J. Solid State Chem.* **2000**, 150, 286.
9. Pelikán P., Košuth M., Biskupič S., Noga J., Straka M., Zajac A., Baňacký P.: *Int. J. Quantum Chem.* **2001**, *84*, 157.
10. An J. M., Picket W. E.: *Phys. Rev. Lett.* **2001**, *86*, 4366.
11. Kortus J., Mazin I. I., Belashchenko K. D., Antropov V. P., Boyer L. L.: *Phys. Rev. Lett.* **2001**, *86*, 4656.
12. Baňacký P.: *Int. J. Quantum Chem.* **2005**, *101*, 131.
13. Boeri L., Cappelluti E., Pietronero L.: *Phys. Rev. B* **2005**, *71*, 012501.
14. Pietronero L., Strassler S., Grimaldi C.: *Phys. Rev. B* **1995**, *52*, 10516.
15. Svrček M., Baňacký P., Zajac A.: *Int. J. Quantum Chem.* **1992**, *43*, 393.
16. Kutzelnigg W.: *Mol. Phys.* **1997**, *90*, 909.
17. Svrček M., Baňacký P., Biskupič S., Noga J, Pelikán P., Zajac A.: *Chem. Phys. Lett.* **1999**, *299*, 151.
18. Lu D. H., Feng D. L., Armitage N. P., Shen K. M., Damascelli A., Kim C., Ronning F., Shen Z. X., Bonn D. A., Liang R., Hardy W. N., Rykov A. I., Tajima S.: *Phys. Rev. Lett.* **2001**, *86*, 4370.
19. Martinez-Samper P., Rodrigo J. G., Rubio-Bollinger G., Suderow M., Vieira S., Lee S., Tajima S.: *Physica C* **2003**, *385*, 233.
20. Szabo P., Samuely P., Kacmarek J., Klein T., Marcus J., Fruchart D., Miraglia S., Mareinit C., Jensen A. G. M.: *Phys. Rev. Lett.* **2001**, *87*, 137005.
21. Svrček M., Baňacký P., Zajac A.: *Int. J. Quantum Chem.* **1992**, *43*, 415.
22. Hor P. H., Meng R. L., Wang Y. Q., Gao L., Hung Z. J., Bechtold J., Forster K., Chu C. W.: *Phys. Rev. Lett.* **1987**, *58*, 1191.
23. Nagamatsu J., Nakagava N., Muranaka T., Zenitani Y., Akimitsu J.: *Nature* **2001**, *410*, 63.
24. Matthias B. T., Gebale T. M., Andres K.: *Science* **1968**, *159*, 530.
25. Lortz L., Wang Y., Tutsch U., Abe S., Meingart C., Popovich P., Knafo W., Schitsevalova N., Pademo Y. B., Junod A.: *Phys. Rev. B* **2006**, *73*, 024512.
26. Xu Y., Zhang L., Cui T., Li Y., Xie Y., Yu W., Ma Y., Zou G.: *Phys. Rev. B* **2007**, *76*, 214103.
27. Schell G., Winter H., Rietchel H., Gompf F.: *Phys. Rev. B* **1982**, *25*, 1589.

28. Calandra M., Kolmogorov A. N., Curtarolo S.: *Phys. Rev. B* **2007**, *75*, 144506.
29. Liu A. Y., Mazin I. I.: *Phys. Rev. B* **2007**, *75*, 064510.
30. Baňacký P.: *Physica C* **2007**, *460–462*, 1115.